MOLECULAR AND CELLULAR BIOLOGY, Nov. 2005, p. 9478–9490 Vol. 25, No. 21
0270-7306/05/$08.00+0 doi:10.1128/MCB.25.21.9478–9490.2005

Constitutive Activation of the pH-Responsive Rim101 Pathway in Yeast Mutants Defective in Late Steps of the MVB/ESCRT Pathway

Michio Hayashi,[1,2] Takaaki Fukuzawa,[1] Hiroyuki Sorimachi,[2,3] and Tatsuya Maeda[1,2]*

Institute of Molecular and Cellular Biosciences, The University of Tokyo, 1-1-1 Yayoi, Bunkyo-ku, Tokyo 113-0032,[1] Department of Enzymatic Regulation for Cell Functions, The Tokyo Metropolitan Institute of Medical Science, 3-18-22 Honkomagome, Bunkyo-ku, Tokyo 113-8613,[3] and CREST, Japan Science and Technology, Kawaguchi 332-0012,[2] Japan

Received 7 February 2005/Returned for modification 31 March 2005/Accepted 5 August 2005

In many fungi, transcriptional responses to alkaline pH are mediated by conserved signal transduction machinery. In the homologous system in *Saccharomyces cerevisiae*, the zinc-finger transcription factor Rim101 is activated under alkaline conditions to regulate transcription of target genes. The activation of Rim101 is exerted through proteolytic processing of its C-terminal inhibitory domain. Regulated processing of Rim101 requires several proteins, including the calpain-like protease Rim13/Cpl1, a putative protease scaffold Rim20, putative transmembrane proteins Rim9, and Rim21/Pal2, and Rim8/Pal3 of unknown biochemical function. To identify new regulatory components and thereby determine the order of action among the components in the pathway, we screened for suppressors of *rim9*Δ and *rim21*Δ mutations. Three identified suppressors—*did4*/*vps2*, *vps24*, and *vps4*—all belonged to "class E" *vps* mutants, which are commonly defective in multivesicular body sorting. These mutations suppress *rim8*, *rim9*, and *rim21* but not *rim13* or *rim20*, indicating that Rim8, Rim9, and Rim21 act upstream of Rim13 and Rim20 in the pathway. Disruption of *DID4*, *VPS24*, or *VPS4*, by itself, uncouples pH sensing from Rim101 processing, leading to constitutive Rim101 activation. Based on extensive epistasis analysis between pathway-activating and -inactivating mutations, a model for architecture and regulation of the Rim101 pathway is proposed.

Microorganisms must regulate gene expression to cope with changes in environmental pH. In many fungi, transcriptional responses to alkaline pH are mediated by conserved signal transduction machinery (59). Extensive studies conducted on the prototypical pathway of *Aspergillus nidulans* have led to many of our current insights into the molecular machinery of homologous pathways (3, 59). In the *A. nidulans* pathway, the zinc-finger transcription factor PacC, is activated at alkaline pH to directly regulate transcription of pH-responsive genes (17, 72). Activation of PacC is exerted through proteolytic processing and removal of its C-terminal inhibitory domain at alkaline pH (21, 50, 55). The processing of PacC requires several proteins called the Pal proteins, whose deficiency causes acidity-mimicking phenotypes (2, 17, 19, 20, 48, 53, 54, 55). A set of dominant mutants of *pacC* that encode C-terminally truncated proteins mimicking the processed form behave as constitutively active mutants (*pacC*^{C}) and cause alkalinity-mimicking phenotypes (17, 55, 72). Because the acidity-mimicking phenotypes of any of the *pal* mutants are suppressed by *pacC*^{C}, the Pal proteins are concluded to constitute a pathway that regulates processing of PacC in response to alkaline pH (2, 17). However, the absence of other alkalinity-mimicking mutants has hindered similar genetic analyses meant to determine the order of action among the Pal proteins in the pathway.

In *Saccharomyces cerevisiae*, the homologous pathway regulates proteolytic processing of Rim101, which is the ortholog of PacC (59). Rim101 was originally identified as a positive regulator for meiotic gene expression (also referred to as Rim1 [68, 69]) and was subsequently shown to be responsible for alkaline pH-responsive gene expression and thereby for adaptation to alkaline conditions (25, 40, 41, 65). Rim101 also is activated by C-terminal proteolytic processing that is stimulated at alkaline pH (44). Several proteins homologous to the Pal proteins in *A. nidulans* are required for this processing, including the calpain-like protease Rim13/Cpl1, a putative protease scaffold Rim20, putative transmembrane proteins Rim9 and Rim21/Pal2, and Rim8/Pal3, a protein of unknown biochemical function (25, 41, 44, 73, 79). Defective mutants in any of these Rim proteins show sensitivity to alkaline conditions, as well as LiCl-containing medium. The latter phenotype is caused by reduced expression of *ENA1*, encoding the cation extrusion pump, whose efficient expression is dependent on Rim101 processing (41). Recently, Rim101 was shown to function as a transcriptional repressor that negatively regulates expression of several target genes, including *NRG1* and *SMP1*; the product of the former is in turn required for repression of *ENA1* (40). Like *A. nidulans* PacC^{C}, C-terminally truncated mutants of Rim101 that mimic the processed form, such as Rim101ΔC531, also behave as constitutively active forms and negate the requirement for Rim13 activity or activity of any of the other Rim proteins needed for Rim101 processing (25, 44; E. Futai and T. Maeda, unpublished data). Therefore, molecular machinery homologous to what operates in *A. nidulans* appears to regulate Rim101 processing in *S. cerevisiae*

* Corresponding author. Mailing address: Institute of Molecular and Cellular Biosciences, The University of Tokyo, 1-1-1 Yayoi, Bunkyo-ku, Tokyo 113-0032, Japan. Phone: 81-3-5841-7820. Fax: 81-3-5841-7899. E-mail: maeda@iam.u-tokyo.ac.jp.

(hereafter referred to as the "Rim101 pathway"). The mechanism by which the pathway executes regulated processing of Rim101, however, is not known, for the primary structures of the constituent components, with the exception of the calpain-like protease Rim13, whose proteolytic activity is essential for the pathway (25), provide little insight into their biochemical functions. Further, phenotypes of mutants defective in these components are indistinguishable from one another. The order of action among the Rim proteins in the pathway has also been difficult to determine, as is the case for the *A. nidulans* pathway. Homologous pathways are widely conserved among other fungal species, including *Yarrowia lipolytica* (27, 42, 73) and *Candida albicans* (18, 43, 61, 62).

Recently, machinery for vacuolar protein sorting was implicated in activation of the Rim101 pathway. Vacuolar sorting is mediated by the concerted action of a set of proteins collectively called vacuolar protein sorting (*VPS*) gene products (31). Among proteins destined for the vacuole, a membrane-bound precursor of carboxypeptidase S (CPS), as well as endocytosed cell surface receptors and transporters destined for vacuolar degradation, are recognized at the endosome and are sorted into multivesicular bodies (MVBs), endosomal structures formed by the invagination and budding of the limiting membrane into the lumen of the compartment (34). After fusion of the MVB with the vacuole, the lumenal vesicles with their cargo proteins are exposed to vacuolar hydrolases for degradation. Sorting of these cargo proteins and formation of the MVB require a group of *VPS* gene products categorized as "class E," which include all components of three protein complexes called ESCRTs (for endosomal sorting complex required for transport): ESCRT-I, -II, and -III. Null mutations in any of the "class E" *VPS* genes commonly result in defective MVB sorting and accumulation of a malformed endosomal structure called the "class E" compartment. As a signal for MVB sorting, many cargo proteins, such as the precursor of CPS and cell surface receptors, are ubiquitinated within cytoplasmically exposed domains. Among the "class E" Vps proteins, the Stp22/Vps23 subunit of the ESCRT-I complex (composed of Stp22, Vps28, and Srn2/Vps37) and Vps27 bind to ubiquitin and thus select ubiquitinated cargo proteins for transport (7, 29, 33, 45, 60, 63, 67). Vps27 also binds the endosomally enriched lipid species phosphatidylinositol 3-phosphate and thereby initiates MVB sorting on the endosomal membrane (15, 35). ESCRT-I is then recruited for MVB sorting through direct interaction with Vps27 and binds to ubiquitinated cargo proteins (35). ESCRT-I then recruits ESCRT-II (composed of Snf8/Vps22, Vps25, and Vps36) onto the endosomal membrane, which in turn initiates assembly and recruitment of ESCRT-III onto the endosomal membrane (6, 47, 82). ESCRT-III is composed of the soluble coiled-coil-containing proteins Did4/Vps2, Vps20, Vps24, and Snf7/Vps32, which are recruited from the cytoplasm to the endosomal membrane, where they oligomerize into the complex (1, 5, 9, 37, 74). ESCRT-III contains two functionally distinct subcomplexes (5). The Vps20-Snf7 subcomplex binds to the endosomal membrane, in part through the myristoyl group of Vps20 (5). The Did4-Vps24 subcomplex binds to the Vps20-Snf7 subcomplex and thereby serves to recruit additional cofactors to the site of protein sorting, such as Vps4, which is an AAA-type ATPase catalyzing dissociation and disassembly of all three ESCRT complexes from the endosomal membrane after sorting is complete, and Doa4, which catalyzes the deubiquitination of cargo proteins to recycle ubiquitin (1, 5, 8, 56). The ESCRT complexes are thus proposed to perform a coordinated cascade of reactions that direct selection and sorting of MVB cargo proteins destined for delivery to the lumen of the vacuole.

A possible link between the Rim101 pathway and MVB sorting was suggested by several observations. For example, in a study of alkaline adaptation in *Y. lipolytica*, *vps28*, together with *rim* homolog mutants, was identified as a mutant in which induction of pH-responsive reporter genes was eliminated, although Rim101 processing in *vps28* cells was not examined (27). In addition, a genome-wide protein interaction analysis suggested that Rim20 interacts with Snf7, and Snf7 in turn interacts with Rim13 (30, 79). Recently, Xu et al. reported that Rim101 processing is deficient in *stp22*Δ, *vps28*Δ, *srn2*Δ, *snf8*Δ, *vps25*Δ, *vps36*Δ, *snf7*Δ, and *vps20*Δ mutants but proficient in other "class E" *vps* mutants (80). Also in *C. albicans*, *snf7*Δ mutants are defective in Rim101 processing and show phenotypes attributed by the defect (39).

Here we screened for suppressors of two mutations, *rim9*Δ and *rim21*Δ, that cause deficiency in putative membrane-associated components of the Rim101 pathway. The three identified suppressors were all found to belong to "class E" *vps* mutations. These mutations cause constitutive activation of the Rim101 pathway by themselves. Based on extensive epistasis analysis between these pathway-activating mutations and pathway-inactivating *rim* and *vps* mutations, a model for the architecture of the Rim101 pathway and its regulation is proposed.

MATERIALS AND METHODS

Molecular genetic methods. Standard *Escherichia coli* and yeast manipulations were performed as described previously (4). *E. coli* strain XL10-Gold (Stratagene, San Diego, CA) was used for plasmid propagation.

Yeast media. Yeast extract-peptone-dextrose (YPD), synthetic dextrose (SD), synthetic complete (SC) dropout, and sporulation media were prepared as described previously (16). SD was supplemented with appropriate auxotrophic requirements. SD and SC were buffered where noted in Results with 50 mM morpholinepropanesulfonic acid and 50 mM morpholineethanesulfonic acid and adjusted to pH 3.5 or 4 with HCl or to pH 5.5, pH 7, or pH 7.5 with NaOH. In order to clone the corresponding genes for the suppressors, SD was supplemented with 7.5 μM erythrosin B (12).

Yeast strains. Yeast strains are listed in Table 1. All strains used were derived in the S288C background (14, 77) except for those used for screening (38). *RIM101* in CH1305 and *RIM9* or *RIM21* in CH1462 were disrupted by replacement with a *kanMX6* cassette amplified by PCR as described previously (46) to generate FI1, FI3, and FI5, respectively. FI10-2d and FI10-5a were constructed by crossing FI1 with FI3. FI11-3c and FI11-13b were constructed by crossing FI1 with FI5.

FM81, FM91, FM201, and FM301 were constructed by replacing *RIM8*, *RIM9*, *RIM20*, and *RIM21* of TM141 with a *HIS3* cassette amplified by PCR as described previously (14). *DID4* in FM81, FM91, FM201, FM301, and MTM100 was disrupted by replacement with *kanMX6* amplified by PCR. The resultant double disruptant strains were backcrossed with TM225 to generate VB181-3a, VB191-11c, VB121-5d, VB131-1a, VB151-5d, and VB101-6b. *VPS24* in TM141, FM81, FM91, FM201, FM301, and MTM100 was disrupted by replacement with *kanMX6* amplified by PCR. The resultant double disruptant strains were backcrossed with TM225 to generate VX101-10a, VX181-6a, VX191-6d, VX121-2c, VX131-5a, and VX151-1c. *VPS4* in TM225 was disrupted by replacement with *kanMX6* amplified by PCR to generate FT11. FT101, FT181, FT191, FT121, FT131, and FT151 were constructed by crossing TM141, FM81, FM91, FM201, FM301, and MTM100 with FT11. *SNF7*, *VPS20*, and *VPS24* in TM225 were disrupted by replacement with *His3MX6* amplified by PCR to generate SG11, VT11, and VX401, respectively. SG101-9b, VB271-26c, and VX271-13d were

TABLE 1. Yeast strains

Strain	Genotype	Source or reference
CH1305	*MAT***a** *ade2 ade3 leu2 ura3 lys2*	38
CH1462	*MATα ade2 ade3 leu2 ura3 his3*	38
FI1	Same as CH1305 except *rim101*::*kanMX6*	This study
FI3	Same as CH1462 except *rim9*::*kanMX6*	This study
FI5	Same as CH1462 except *rim21*::*kanMX6*	This study
FI10-2d	Same as CH1305 except *rim101*::*kanMX6 rim9*::*kanMX6*	This study
FI10-5a	Same as CH1462 except *rim101*::*kanMX6 rim9*::*kanMX6*	This study
FI11-3c	Same as CH1305 except *rim101*::*kanMX6 rim21*::*kanMX6*	This study
FI11-13b	Same as CH1462 except *rim101*::*kanMX6 rim21*::*kanMX6*	This study
A6	Same as FI10-5a except *did4-H1*	This study
A108-9a	Same as FI10-5a except *vps24-H1*	This study
TM141	*MAT***a** *ura3-52 leu2Δ1 trp1Δ63 his3Δ200*	Lab stock (77)
TM225	*MATα ura3-52 leu2Δ1 his3Δ200 lys2Δ202*	FY838 (77)
MTM100	*MAT***a** *ura3-52 leu2Δ1 trp1Δ63 rim13*::*URA3*	25
FM81	Same as TM141 except *rim8*::*HIS3*	This study
FM91	Same as TM141 except *rim9*::*HIS3*	This study
FM201	Same as TM141 except *rim20*::*HIS3*	This study
FM301	Same as TM141 except *rim21*::*HIS3*	This study
VB101-6b	Same as TM141 except *did4*::*kanMX6*	This study
VB181-3a	Same as TM141 except *rim8*::*HIS3 did4*::*kanMX6*	This study
VB191-11c	Same as TM141 except *rim9*::*HIS3 did4*::*kanMX6*	This study
VB121-5d	Same as TM141 except *rim20*::*HIS3 did4*::*kanMX6*	This study
VB131-1a	Same as TM141 except *rim21*::*HIS3 did4*::*kanMX6*	This study
VB151-5d	Same as TM141 except *rim13*::*URA3 did4*::*kanMX6*	This study
VB271-26c	Same as TM141 except *snf7*::*His3MX6 did4*::*kanMX6*	This study
VB321-1a	Same as TM141 except *vps20*::*His3MX6 did4*::*kanMX6*	This study
VX101-10a	Same as TM141 except *vps24*::*kanMX6*	This study
VX181-6a	Same as TM141 except *rim8*::*HIS3 vps24*::*kanMX6*	This study
VX191-6d	Same as TM141 except *rim9*::*HIS3 vps24*::*kanMX6*	This study
VX121-2c	Same as TM141 except *rim20*::*HIS3 vps24*::*kanMX6*	This study
VX131-5a	Same as TM141 except *rim21*::*HIS3 vps24*::*kanMX6*	This study
VX151-1c	Same as TM141 except *rim13*::*URA3 vps24*::*kanMX6*	This study
VX271-13d	Same as TM141 except *snf7*::*His3MX6 vps24*::*kanMX6*	This study
VX321-4d	Same as TM141 except *vps20*::*His3MX6 vps24*::*kanMX6*	This study
FT11	Same as TM225 except *vps4*::*kanMX6*	This study
FT101	Same as TM141 except *vps4*::*kanMX6*	This study
FT181	Same as TM141 except *rim8*::*HIS3 vps4*::*kanMX6*	This study
FT191	Same as TM141 except *rim9*::*HIS3 vps4*::*kanMX6*	This study
FT121	Same as TM141 except *rim20*::*HIS3 vps4*::*kanMX6*	This study
FT131	Same as TM141 except *rim21*::*HIS3 vps4*::*kanMX6*	This study
FT151	Same as TM141 except *rim13*::*URA3 vps4*::*kanMX6*	This study
SG11	Same as TM225 except *snf7*::*His3MX6*	This study
SG101-9b	Same as TM141 except *snf7*::*His3MX6*	This study
VT11	Same as TM225 except *vps20*::*His3MX6*	This study
VT101-6d	Same as TM141 except *vps20*::*His3MX6*	This study
VX401	Same as TM225 except *vps24*::*His3MX6*	This study
BY4741	*MAT***a** *ura3Δ0 leu2Δ0 his3Δ1 met15Δ0*	Open Biosystems (14)
3416	Same as BY4741 except *stp22*::*kanMX4*	Open Biosystems (78)
2763	Same as BY4741 except *vps28*::*kanMX4*	Open Biosystems (78)
2826	Same as BY4741 except *snf8*::*kanMX4*	Open Biosystems (78)
2580	Same as BY4741 except *vps25*::*kanMX4*	Open Biosystems (78)
5325	Same as BY4741 except *vps36*::*kanMX4*	Open Biosystems (78)
VV7-2c	*MAT***a** *ura3 leu2 his3 met15Δ0 vps24*::*His3MX6*	This study
VV3-3c	*MAT***a** *ura3 leu2 his3 met15Δ0 stp22*::*kanMX4*	This study
VV3-9b	*MAT***a** *ura3 leu2 his3 met15Δ0 stp22*::*kanMX4 vps24*::*His3MX6*	This study
VV7-10d	*MAT***a** *ura3 leu2 his3 met15Δ0 vps28*::*kanMX4*	This study
VV7-7b	*MAT***a** *ura3 leu2 his3 met15Δ0 vps28*::*kanMX4 vps24*::*His3MX6*	This study
VV11-14a	*MAT***a** *ura3 leu2 his3 met15Δ0 snf8*::*kanMX4*	This study
VV11-3a	*MAT***a** *ura3 leu2 his3 met15Δ0 snf8*::*kanMX4 vps24*::*His3MX6*	This study
VV15-9c	*MAT***a** *ura3 leu2 his3 met15Δ0 vps25*::*kanMX4*	This study
VV15-4b	*MAT***a** *ura3 leu2 his3 met15Δ0 vps25*::*kanMX4 vps24*::*His3MX6*	This study
VV19-10a	*MAT***a** *ura3 leu2 his3 met15Δ0 vps36*::*kanMX4*	This study
VV19-16d	*MAT***a** *ura3 leu2 his3 met15Δ0 vps36*::*kanMX4 vps24*::*His3MX6*	This study

constructed by crossing VB101-6b and VX101-10a with SG11. VT101-6d, VB321-1a, and VX321-4d were constructed by crossing VB101-6b and VX101-10a with VT11. All gene disruptions constructed with *kanMX6* or *His3MX6* cassettes were confirmed by Southern analyses.

The *stp22*Δ (strain 3416), *vps28*Δ (strain 2763), *snf8*Δ (strain 2826), *vps25*Δ (strain 2580), *vps36*Δ (strain 5325), and parental (strain BY4741) strains were obtained from Open Biosystems (Huntsville, AL) (14, 78). The authenticity of each disruptant was confirmed as follows. These mutant strains exhibited temperature-sensitive growth and LiCl-sensitive phenotypes (data not shown). Plasmids containing the corresponding wild-type alleles were cloned and found to complement both phenotypes of the respective disruptants (data not shown). These results indicate that in each of above strains, the correct gene had been disrupted.

VV3-3c, VV3-9b, VV15-9c, VV15-4b, VV7-2c, VV7-10d, VV7-7b, VV11-14a, VV11-3a, VV19-10a, and VV19-16d were constructed by crossing strains 3416, 2580, 2763, 2826, and 5325 with VX401.

Plasmids. pRIM101-2, an *RIM101* plasmid with a NotI site introduced upstream of the first codon, has been described (25). Oligonucleotides encoding three tandem copies of the hemagglutinin (3× HA) epitope were inserted into the NotI site. The resultant *3HA-RIM101* fragment (2.1 kb, BamHI-EcoRI) and an *ADE3* fragment (3.7 kb, BamHI-NheI) were inserted into the BamHI-EcoRI sites and the XbaI site of the pRS415 polylinker, respectively, to construct pFI1.

pAS416 was obtained from a YCp50 yeast genomic library as a plasmid rescuing the slow-growth phenotype of a *did4* mutant (A6). Formation of larger and whiter colonies on SD plates containing erythrosin B was used as rescue criteria. pAS416 was found to harbor a 3.8-kb insert containing *DID4*. A 2.5-kb HindIII fragment containing *DID4* and a portion of vector sequence was subcloned into the HindIII site of YCp50 to generate pAS4163.

pAS31 was obtained from the YCp50 yeast genomic library as a plasmid rescuing the slow-growth of a *vps24* mutant (A108-9a), as described for *DID4*. The plasmid was found to harbor a 5.1-kb insert containing *VPS24*. A 1.7-kb ClaI fragment containing *VPS24* was subcloned into the ClaI site of YCp50 to generate pAS311.

A 1.1-kb HindIII fragment containing *URA3* was inserted in pRS415 with modified multiple cloning sites to obtain pTB554. Immediately upstream of the initiation codon of *URA3* on pTB554, a 1.0-kb PCR product upstream of *YPL277C* containing its promoter was inserted by homologous recombination to construct pAT003.

Screening for suppressors. FI10-2d, FI10-5a, FI11-3c, and FI11-13b transformed with pFI1 were mutagenized with ethyl methanesulfonate as described previously (16) (viability 30 to 40%), diluted, plated on YPD plates containing 0.16 or 0.21 M LiCl, and incubated for a week. Nonsectoring "red-only" colonies were selected and retested for the phenotype by streaking onto YPD plates containing 0.21 M LiCl. Candidate clones were retested on the same plates after incubation on YPD plates for 1 day to promote plasmid loss. To exclude mutants that restored LiCl tolerance due to activating mutations in pFI1 plasmid-borne *RIM101*, the plasmid was cured from each mutant and, after retransformation with pFI1, mutants were retested on the same plates. Finally, by Western blotting with an anti-HA antibody, mutants harboring processed HA-Rim101 were selected.

Detection of HA epitope-tagged Rim101. Cells transformed with pFI1 were precultured in SD, inoculated in YPD at an optical density at 600 nm (OD_{600}) of ca. 0.4, and incubated for 4 h. Cells were collected, washed with 1 mM phenylmethylsulfonyl fluoride (this extra washing step is only for the experiments in Fig. 2A, 3A, and 4A), suspended in Laemmli sample buffer, and boiled for 5 min. Samples were then cooled on ice and vortexed with glass beads for 30 s eight times with 30-s intervals on ice. Cell lysates corresponding to OD of 0.5 were boiled for 1 min and subjected to Western blotting with the anti-HA monoclonal antibody 12CA5 and IRDye-conjugated anti-mouse antibody (Rockland, Gilbertsville, PA). To detect actin for a loading control, the anti-actin monoclonal antibody C4 (ICN, Aurora, OH) was used as a primary antibody. Signals were detected by using the infrared imaging system Odyssey (LI-COR, Lincoln, NE) according to the manufacturer's instructions. For the experiments in Fig. 2A, cells were precultured to late log phase (OD = 0.6 to 1) in SD at pH 5.5, inoculated in each buffered SD medium at an OD of 1, and harvested after 30 min. Sample preparation and Western blotting were performed as described above.

RESULTS

Screening for suppressors of *rim9*Δ or *rim21*Δ. To identify new regulatory components in the Rim101 pathway and thus determine the order of action among the components in the pathway, we conducted a screen for mutations that suppressed the phenotypes of disruption alleles of *RIM9* and *RIM21*. Rim9 and Rim21 are putative membrane proteins and thus are more likely to function upstream in the pathway (44, 73). Our initial attempts to isolate suppressors of *rim9*Δ and *rim21*Δ were, however, impeded by bypass suppressors. The screen for suppressors selected mutants whose growth in the presence of LiCl was restored, although none of the isolated mutants restored Rim101 processing (data not shown). It is likely that in these mutants LiCl tolerance was acquired through other mechanisms that also activate *ENA1* expression. To isolate Rim101 pathway-specific suppressors that restored LiCl tolerance through restoration of Rim101 processing, the original screen was redesigned.

For clarity, only the screen for *rim9*Δ suppressors is described. Parental strains were constructed by disrupting both *RIM9* and *RIM101* in a pair of *ade2 ade3* host strains and then transforming them with the screening plasmid pFI1, harboring HA-epitope-tagged *RIM101* and *ADE3*, to facilitate a colony color assay (38). The parental strains had the overall genotype of *rim9*Δ and were therefore sensitive to LiCl. Suppressors were then sought that restored wild-type tolerance to LiCl from these parental strains. Among the mutants expected to be isolated, uninteresting bypass suppressors that restored LiCl tolerance independently of Rim101 processing would not require the pFI1 plasmid for the suppression and thus were expected to form white colonies or red colonies with many white sectors on plates containing LiCl. In contrast, the sought-after Rim101 pathway-specific suppressors would require pFI1 for the suppression and therefore were expected to form nonsectoring red colonies on plates containing LiCl. In addition, the intended pathway-specific suppressors were expected to permit formation of white or sectoring colonies on plates that did not contain LiCl because pFI1 would not then be required. This feature was used to exclude mutants that retained pFI1 for reasons other than a dependence on Rim101 for LiCl tolerance. Suppressors that restored LiCl tolerance due to activating mutations in pFI1-encoded Rim101, such as truncation of the C terminus, were then excluded by retesting the LiCl tolerance of candidate mutants after once curing the screening plasmids from them and then reintroducing genuine pFI1 by transformation. Finally, restoration of Rim101 processing was examined by Western analysis. Similar screening was also performed for suppressors of *rim21*Δ.

Parental strains were mutagenized with ethyl methanesulfonate treatment to a survival rate of 30 to 40%. Nineteen mutants were obtained that harbored *rim9*Δ suppressors restoring both LiCl tolerance and Rim101 processing among a total of 5.6×10^6 clones (Fig. 1A and B). All of the mutations were found to be recessive and were classified into two complementation groups: A and B consisting of 12 and 7 representatives, respectively. Mutants in both complementation groups commonly exhibited slow growth on SD plates and formed colonies that stained darker red than parental strains on SD plates containing the red vital dye, erythrosin B, which accumulates in dead cells (data not shown). Plasmids that restored growth on SD plates, and that also restored defective Rim101 processing were isolated from a wild-type genomic library constructed in YCp50. Subcloning of the isolated plasmids identified *DID4*/

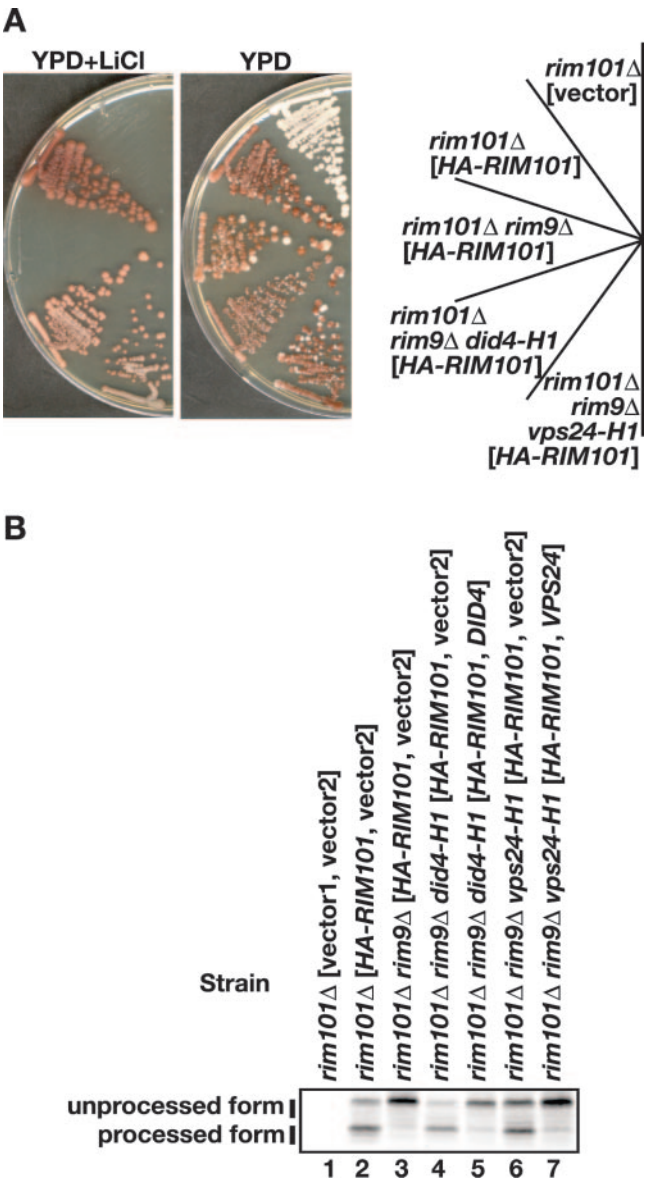

FIG. 1. Screening for *rim9*Δ suppressors. (A) LiCl sensitivity caused by *rim9*Δ is suppressed by *did4* and *vps24*. The *rim101*Δ strain (FI1) transformed with pFI1, a low-copy-number plasmid carrying *HA-RIM101* and *ADE3*, formed red-only, nonsectoring colonies, whereas the same strain carrying pRS415 (vector) failed to grow on an LiCl-containing plate. The red-only, nonsectoring colony morphology indicated that LiCl tolerance was plasmid dependent. The parental strain for the screening, *rim101*Δ *rim9*Δ (FI10-5a) transformed with pFI1, failed to grow on LiCl-containing medium. Isolated LiCl-tolerant suppressor strains, *rim101*Δ *rim9*Δ *did4-H1* (A6) and *rim101*Δ *rim9*Δ *vps24-H1* (A108-9a), both transformed with pFI1, formed red-only, nonsectoring colonies on a plate containing LiCl because their LiCl tolerance was plasmid dependent. They formed white or sectoring colonies on a plate that did not contain LiCl because pFI1 was not then required. Cells were streaked on YPD and on YPD containing 0.21 M LiCl plates and incubated at 30°C for 11 days. (B) Defective Rim101 processing caused by *rim9*Δ is suppressed by *did4* and *vps24*. The strains used in panel A were transformed with pRS415 (vector1) or pFI1, in combination with the empty YCp50 vector (vector2), pAS4163, a low-copy-number plasmid carrying *DID4*, or pAS311, a low-copy-number plasmid carrying *VPS24*, as indicated. Transformants were precultured in SD to logarithmic phase and then transferred to YPD. After a 3-h incubation, cells were collected, and cell lysates were prepared. Processed and unprocessed forms of HA-Rim101 (indicated) were detected by Western blotting with an anti-HA antibody.

VPS2 (1) and *VPS24* (9) as the genes corresponding to group A and B mutants, respectively (Fig. 1B). Phenotypes of the double mutants constructed using *rim9*Δ, and *did4*Δ or *vps24*Δ confirmed the conclusions (see below).

In the same manner, 10 mutants were obtained that harbored *rim21*Δ suppressors among a total of 1.5×10^7 clones. One mutation was found to be dominant, and the other nine were found to be recessive (data not shown). Analysis of the dominant mutation will be reported elsewhere. The recessive mutations obtained were classified into three complementation groups: C, D, and E, consisting of five, three, and one representative, respectively. As the mutants harboring the *rim9*Δ suppressors, these mutants also exhibited slow growth on SD plates and formed colonies that stained darker red on SD plates containing erythrosin B. Transformation of representative mutants of these groups with plasmids harboring either of *DID4* or *VPS24* revealed that the phenotypes of group C and E mutants were rescued by *VPS24* and *DID4*, respectively (data not shown). Cloning of the gene that rescued group D mutants identified *VPS4* (8). To summarize, these results identified *VPS24*, *VPS4*, and *DID4* as the genes corresponding to group C, D, and E mutants, respectively. Phenotypes of double mutants constructed using *rim21*Δ and *vps24*Δ, *vps4*Δ, or *did4*Δ confirmed our conclusions (see below).

***did4*Δ, *vps24*Δ, and *vps4*Δ mutations constitutively activate the Rim101 pathway.** To analyze the functions of Did4, Vps24, and Vps4 in the Rim101 pathway, *DID4*, *VPS24*, and *VPS4* disruptants were constructed in the S288C isogenic background, and processing of HA-Rim101 was monitored by Western blotting. When wild-type cells were transferred to an acidic condition (pH 3.5), HA-Rim101 was mostly unprocessed (Fig. 2A, lane 2). On the other hand, when cells were transferred to an alkaline condition (pH 7.5), most HA-Rim101 was processed (Fig. 2A, lane 4). The degree of HA-Rim101 processing is between those of two conditions at pH 5.5 (Fig. 2A, lane 3). The accumulation of processed Rim101 under alkaline conditions and unprocessed form under acidic conditions are in good agreement with previous observations (44).

In *did4*Δ mutants transferred to any condition of pH 3.5, 5.5, or 7.5, most HA-Rim101 was processed (Fig. 2A, lanes 5 to 7) as in wild-type cells at pH 7.5 (Fig. 2A, lane 4). This was also the case in *vps24*Δ mutants (Fig. 2A, lanes 8 to 10). These results indicate that in *did4*Δ and *vps24*Δ mutants, HA-Rim101 processing occurs constitutively in a medium pH-independent manner and that both *did4*Δ and *vps24*Δ mutations constitutively activate the Rim101 pathway. Also in *vps4*Δ mutants, HA-Rim101 processing was constitutive irrespective of medium pH (Fig. 2A, lanes 11 to 13), although the degree of processing was less pronounced than in *did4*Δ and *vps24*Δ mutants. These results indicate that in *vps4*Δ mutants, HA-Rim101 processing occurs constitutively at a low level in a medium pH-independent manner and that a *vps4*Δ mutation moderately activates the Rim101 pathway.

Constitutive activation of the Rim101 pathway in *did4*Δ, *vps24*Δ, and *vps4*Δ mutants was confirmed by using a Rim101-responsive transcriptional reporter. Lamb and Mitchell identified several target genes for direct repression by Rim101, among which, *YPL277C* was most significantly upregulated by deficiency of the Rim101 pathway (40). Therefore, a reporter plasmid was constructed by connecting the promoter segment

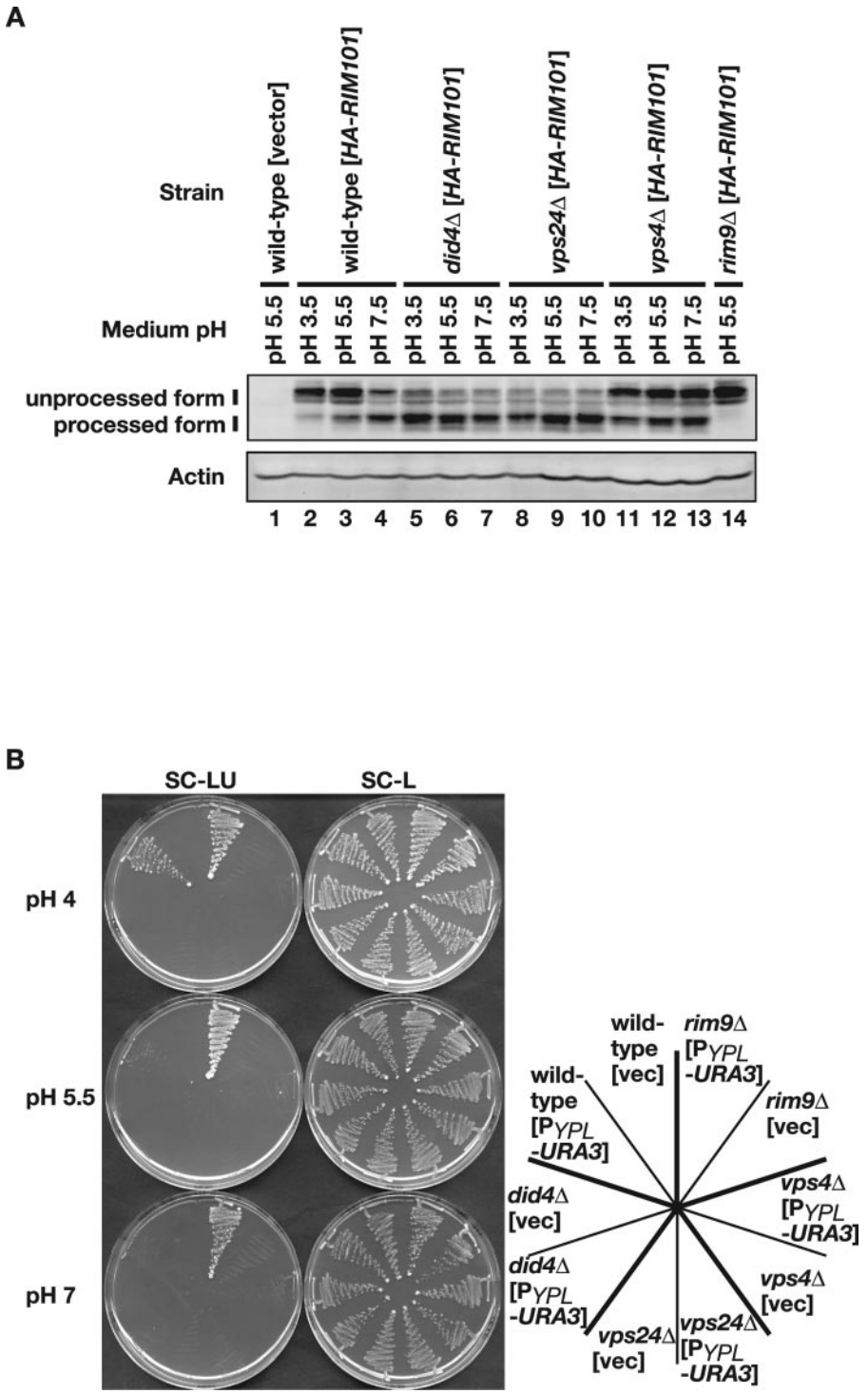

FIG. 2. *did4*Δ, *vps24*Δ, and *vps4*Δ mutations activate the Rim101 pathway constitutively. (A) Constitutive and pH-independent processing of Rim101 is observed in *did4*Δ, *vps24*Δ, and *vps4*Δ mutants. HA-Rim101 was expressed from pFI1 in wild-type (TM141), *did4*Δ (VB101-6b), *vps24*Δ (VX101-10a), *vps4*Δ (FT101), and *rim9*Δ (FM91) strains. Cells were grown to logarithmic phase in SD buffered at pH 5.5 and then transferred to SD buffered at pH 3.5, 5.5, or 7.5 for 30 min. Cell lysates were prepared, and processed and unprocessed forms of HA-Rim101 (indicated) were detected as described in the legend to Fig. 1. Actin Western blotting was used as a loading control. (B) Constitutive and pH-independent repression of the Rim101-repressible *YPL277C* promoter is observed in *did4*Δ, *vps24*Δ, and *vps4*Δ mutants. The $P_{YPL277C}$-*URA3* reporter plasmid pAT003 (P_{YPL}-*URA3*) or pRS415 (vec) was introduced in the strains used in panel A. The transformants were streaked on SC-LU and SC-L plates adjusted to indicated pH and then incubated at 30°C for 3 days.

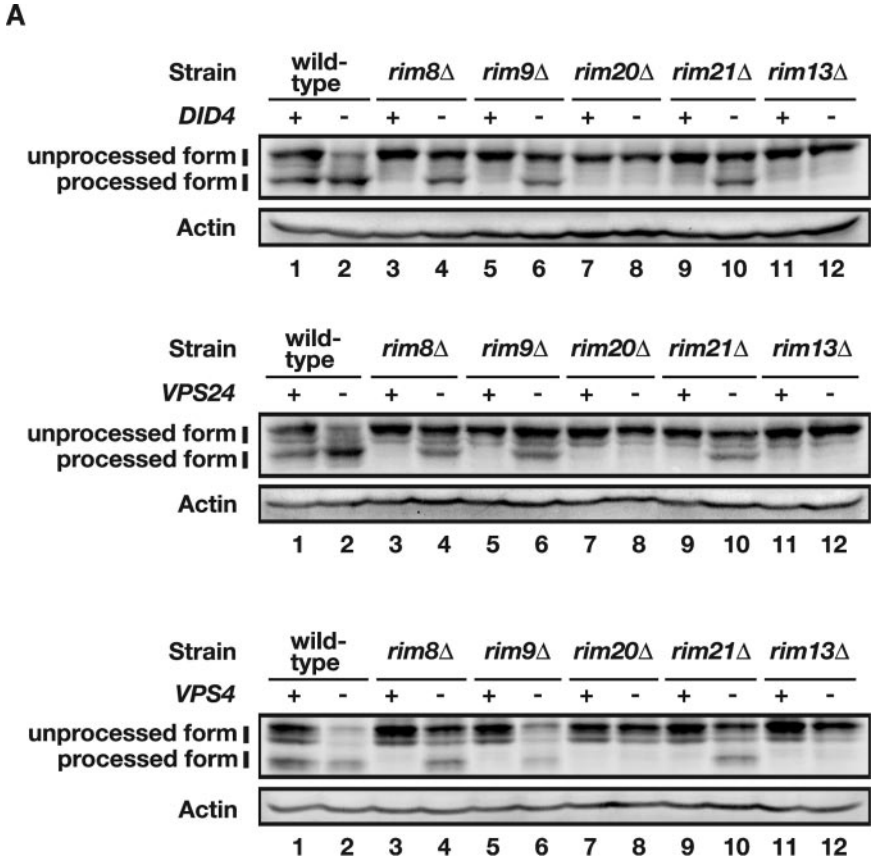

FIG. 3. *did4*Δ, *vps24*Δ, and *vps4*Δ mutations suppress *rim8*Δ, *rim9*Δ, and *rim21*Δ but not *rim20*Δ or *rim13*Δ. (A) *did4*Δ, *vps24*Δ, and *vps4*Δ mutations suppress defective Rim101 processing of *rim8*Δ, *rim9*Δ, and *rim21*Δ mutants but not that of *rim20*Δ and *rim13*Δ mutants. HA-tagged Rim101 was expressed from pFI1 in wild-type (TM141), *rim8*Δ (FM81), *rim9*Δ (FM91), *rim20*Δ (FM201), *rim21*Δ (FM301), and *rim13*Δ (MTM100) strains and their *did4*Δ (top panel), *vps24*Δ (middle panel), and *vps4*Δ (bottom panel) derivatives: *did4*Δ (VB101-6b), *rim8*Δ *did4*Δ (VB181-3a), *rim9*Δ *did4*Δ (VB191-11c), *rim20*Δ *did4*Δ (VB121-5d), *rim21*Δ *did4*Δ (VB131-1a), *rim13*Δ *did4*Δ (VB151-5d), *vps24*Δ (VX101-10a), *rim8*Δ *vps24*Δ (VX181-6a), *rim9*Δ *vps24*Δ (VX191-6d), *rim20*Δ *vps24*Δ (VX121-2c), *rim21*Δ *vps24*Δ (VX131-5a), *rim13*Δ *vps24*Δ (VX151-1c), *vps4*Δ (FT101), *rim8*Δ *vps4*Δ (FT181), *rim9*Δ *vps4*Δ (FT191), *rim20*Δ *vps4*Δ (FT121), *rim21*Δ *vps4*Δ (FT131), and *rim13*Δ *vps4*Δ (FT151) strains. Processed and unprocessed forms of HA-Rim101 (indicated) were detected as described in the legend to Fig. 1. Actin Western blotting was used as a loading control. +, intact; −, deleted. (B) *did4*Δ, *vps24*Δ, and *vps4*Δ mutations suppress the LiCl sensitivity of *rim8*Δ, *rim9*Δ, and *rim21*Δ mutants but do not suppress that of the *rim20*Δ or *rim13*Δ mutant. The strains used in panel A were streaked on YPD and YPD containing 0.32 M LiCl plates and incubated at 30°C for 5 (lower panel) or 6 (upper and middle panels) days.

of *YPL277C* to immediately upstream of the initiation codon of *URA3*. When the reporter plasmid was introduced into wild-type cells, cells did grow on media lacking uracil at pH 4, where processing of Rim101 was kept impeded, but not at pH 7, where processing of Rim101 was stimulated (Fig. 2B). Cell grew poorly at pH 5.5 (Fig. 2B). Furthermore, when introduced into *rim9*Δ cells, in which processing of Rim101 did not occur irrespective of pH conditions, cells did grow on media lacking uracil at any of the three pH levels (Fig. 2B). These observations indicate that the reporter is effective in monitoring activity of Rim101. When the reporter plasmid was introduced into *did4*Δ, *vps24*Δ, and *vps4*Δ mutants, cells did not grow on media lacking uracil at any of the pH conditions examined (Fig. 2B). This result again shows that Rim101 is kept active irrespective of pH conditions in these three mutants.

Epistasis relationship between *rim* mutations and *did4*, *vps24*, or *vps4*. We then examined whether *did4*Δ, *vps24*Δ, or *vps4*Δ were able to suppress *rim8*Δ, *rim9*Δ, *rim20*Δ, *rim21*Δ, or *rim13*Δ. *rim8*Δ, *rim9*Δ, *rim20*Δ, *rim21*Δ, and *rim13*Δ mutants were defective in HA-Rim101 processing (Fig. 3A, lanes 3, 5, 7, 9, and 11) and sensitive to LiCl (Fig. 3B) as described previously. The double mutants *rim8*Δ *did4*Δ, *rim9*Δ *did4*Δ, and *rim21*Δ *did4*Δ were capable of HA-Rim101 processing (Fig. 3A, upper panel, lanes 4, 6, and 10) and tolerant of LiCl (Fig. 3B). These observations indicate that *rim8*Δ, *rim9*Δ, and *rim21*Δ were suppressed by *did4*Δ. In contrast, the double mutants *rim20*Δ *did4*Δ and *rim13*Δ *did4*Δ were defective in HA-Rim101 processing (Fig. 3A, upper panel, lanes 8 and 12) and sensitive to LiCl (Fig. 3B, upper panel), indicating that *rim20*Δ and *rim13*Δ were not suppressed by *did4*Δ. This was also the case for the double mutants with *vps24*Δ (Fig. 3A, middle panel, lanes 4, 6, 8, 10, and 12, and Fig. 3B, middle panel) and *vps4*Δ (Fig. 3A, lower panel, lanes 4, 6, 8, 10 and 12, and Fig. 3B, lower panel). These observations indicate that *rim8*Δ, *rim9*Δ, and *rim21*Δ were suppressed but that *rim20*Δ and *rim13*Δ were not suppressed by *vps24*Δ or *vps4*Δ, although *vps4* mutations were not isolated in our screen for suppressors

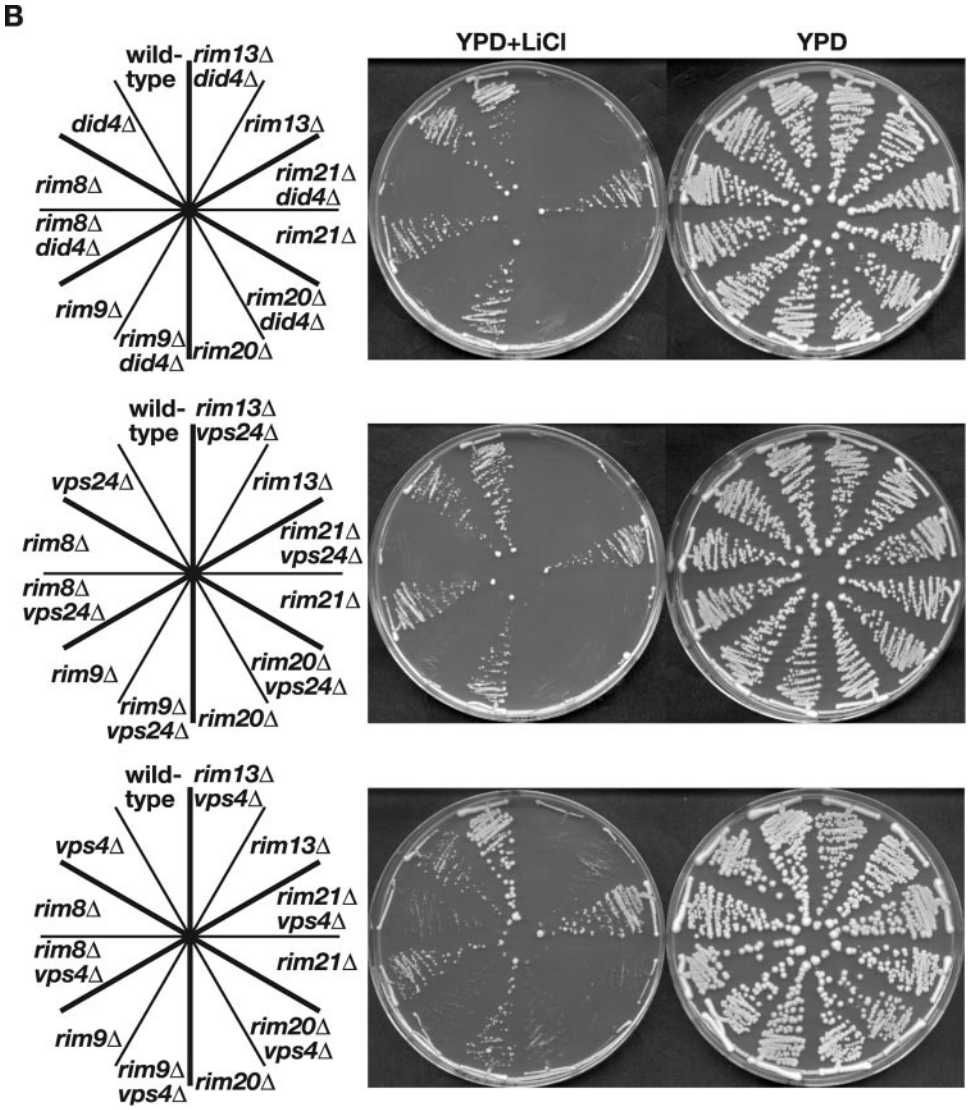

FIG. 3—*Continued.*

of *rim9*Δ. The observations that *rim20* and *rim13* were epistatic to *did4*, *vps24*, and *vps4*, whereas *did4*, *vps24*, and *vps4* were epistatic to *rim8*, *rim9*, and *rim21* provide the genetic evidence that Rim8, Rim9, and Rim21 function upstream of Rim20 and Rim13 in the Rim101 pathway.

Relative to the double mutants *rim8*Δ *did4*Δ, *rim9*Δ *did4*Δ, *rim21*Δ *did4*Δ, *rim8*Δ *vps24*Δ, *rim9*Δ *vps24*Δ, and *rim21*Δ *vps24*Δ, HA-Rim101 processing was more pronounced in *did4*Δ and *vps24*Δ mutants (Fig. 3A, upper and middle panels, lanes 2, 4, 6, and 10). These results indicate that even in *did4*Δ and *vps24*Δ mutants, Rim8, Rim9, and Rim21 still function to facilitate Rim101 processing (see Discussion).

Epistasis relationship between the Rim101 pathway-inactivating ESCRT mutations and *did4* or *vps24*. Recently, it is reported that ESCRT-I components Stp22, Vps28, and Srn2, ESCRT-II components Snf8, Vps25, and Vps36, and ESCRT-III components Snf7 and Vps20 are required for Rim101 processing, just as are Rim8, Rim9, Rim13, Rim20, and Rim21 (80). Our own independent analysis had reached conclusions largely consistent with these results, with the sole exception of Srn2, which was dispensable for HA-Rim101 processing and LiCl tolerance in our analysis (see Discussion). We then examined whether *did4*Δ or *vps24*Δ was able to suppress phenotypes of mutants defective in these ESCRT components with respect to HA-Rim101 processing and LiCl tolerance.

*stp22*Δ, *vps28*Δ, *snf8*Δ, *vps25*Δ, *vps36*Δ, *snf7*Δ, and *vps20*Δ mutants were commonly defective in HA-Rim101 processing (Fig. 4A, lanes 3, 5, 7, 9, and 11, and Fig. 4C, lanes 4 and 7) and sensitive to LiCl (Fig. 4B and 4D) as described above. In contrast, *stp22*Δ *vps24*Δ and *vps28*Δ *vps24*Δ double mutants were capable of HA-Rim101 processing (Fig. 4A, lanes 4 and 6) and tolerant of LiCl (Fig. 4B). Similarly, an *snf8*Δ *vps24*Δ double mutant was moderately proficient in HA-Rim101 processing (Fig. 4A, lane 8) and somewhat tolerant of LiCl (Fig. 4B). *vps25*Δ *vps24*Δ, *vps36*Δ *vps24*Δ, *snf7*Δ *vps24*Δ, and *vps20*Δ *vps24*Δ double mutants were, however, defective in HA-Rim101 processing (Fig. 4A, lanes 10 and 12, and Fig. 4D, lanes 6 and 9) and sensitive to LiCl (Fig. 4B and 4D). *snf7*Δ

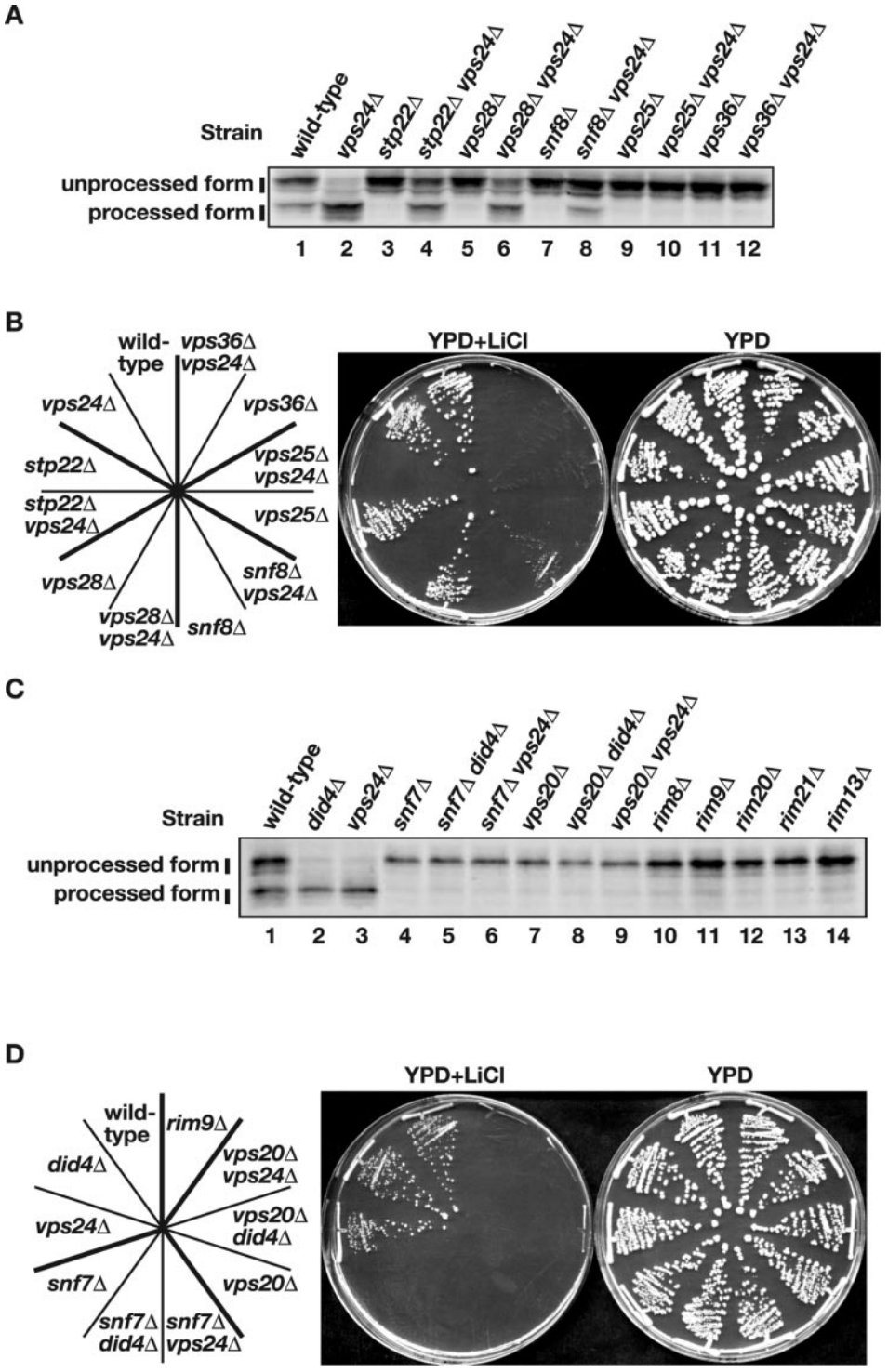

FIG. 4. Epistasis tests between the Rim101 pathway-inactivating ESCRT mutations and *did4* or *vps24*. (A) Defective Rim101 processing of *stp22*Δ and *vps28*Δ mutants is suppressed by *vps24*Δ, that of an *snf8*Δ mutant is suppressed moderately, and that of *vps25*Δ and *vps36*Δ mutants is not suppressed by *vps24*Δ. HA-tagged Rim101 was expressed from pFI1 in wild-type (BY4741), *stp22*Δ (VV3-3c), *vps28*Δ (VV7-10d), *snf8*Δ (VV11-14a), *vps25*Δ (VV15-9c), and *vps36*Δ (VV19-10a) strains and their *vps24*Δ derivatives: *vps24*Δ (VV7-2c), *stp22*Δ *vps24*Δ (VV3-9b), *vps28*Δ *vps24*Δ (VV7-7b), *snf8*Δ *vps24*Δ (VV11-3a), *vps25*Δ *vps24*Δ (VV15-4b), and *vps36*Δ *vps24*Δ (VV19-16d) strains. Processed and unprocessed forms of HA-Rim101 (indicated) were detected as described in the legend to Fig. 1. (B) The LiCl sensitivity of *stp22*Δ and *vps28*Δ mutants is suppressed by *vps24*Δ, that of an *snf8*Δ mutant is suppressed moderately, and that of *vps25*Δ and *vps36*Δ mutants is not suppressed by *vps24*Δ. The strains used in panel A were streaked on YPD and YPD containing 0.32 M LiCl plates and incubated at 30°C for 6 days. (C) Defective Rim101 processing of *snf7*Δ and *vps20*Δ mutants is not suppressed by *did4*Δ or *vps24*Δ. HA-tagged Rim101 was expressed from pFI1 in wild-type (TM141), *snf7*Δ (SG101-9b), and *vps20*Δ (VT101-6d) strains and their *did4*Δ and *vps24*Δ derivatives: *did4*Δ (VB101-6b), *vps24*Δ (VX101-10a), *snf7*Δ *did4*Δ(VB271-26c), *snf7*Δ *vps24*Δ (VX271-13d), *vps20*Δ *did4*Δ (VB321-1a), and *vps20*Δ *vps24*Δ (VX321-4d), *rim8*Δ (FM81), *rim9*Δ (FM91), *rim20*Δ (FM201), *rim21*Δ (FM301), and *rim13*Δ (MTM100) strains. Processed and unprocessed forms of HA-Rim101 (indicated) were detected as described in the legend to Fig. 1. (D) The LiCl sensitivity of *snf7*Δ and *vps20*Δ mutants is not suppressed by *did4*Δ or *vps24*Δ. The indicated strains used in panel C were streaked on YPD and YPD containing 0.32 M LiCl plates and incubated at 30°C for 5 days.

*did4*Δ and *vps20*Δ *did4*Δ double mutants were also defective in HA-Rim101 processing (Fig. 4C, lanes 5 and 8) and sensitive to LiCl (Fig. 4D).

These results can be summarized as follows. Both defective Rim101 processing and LiCl sensitivity caused by ESCRT-I mutations *stp22*Δ and *vps28*Δ were suppressed by *vps24*Δ, those caused by ESCRT-II mutation *snf8*Δ were moderately suppressed, and those caused by ESCRT-II mutations *vps25*Δ and *vps36*Δ and ESCRT-III mutations *snf7*Δ and *vps20*Δ were not suppressed by *vps24*Δ.

DISCUSSION

New mutants that exhibit constitutive activation of the Rim101 pathway. As of this writing, the only pathway-activating mutants that have been reported in the Rim101 pathway harbor dominant alleles of *RIM101* encoding proteins with C-terminal truncations that mimic proteolytic processing (44). In the current study, we identified *did4*, *vps24*, and *vps4* as pathway-activating mutants of the Rim101 pathway that are alkaline-mimicking. In our experimental system, most of the HA-Rim101 pool in wild-type cells remained unprocessed under acidic conditions (pH 3.5). The extent of processing increased as medium pH rose, and under alkaline conditions (pH 7.5) most of the HA-Rim101 pool was processed. In *did4* or *vps24* mutants, constitutive proteolytic processing of Rim101 was observed that occurs irrespective of medium pH. The extent of the processing was comparable to that induced in wild-type cells under alkaline conditions. In addition, *did4* and *vps24* mutations were found to suppress defective Rim101 processing in *rim8*, *rim9*, and *rim21* mutants. Similarly, in *vps4* mutants, Rim101 processing was observed even under conditions of acidic pH, although the extent of processing was less than in *did4* or *vps24* mutants. Consistent with this, *rim8*, *rim9*, and *rim21* were also modestly suppressed by *vps4*.

Order of action among the Rim proteins and the ESCRT components. Identification of *did4*, *vps24*, and *vps4* as Rim101 pathway-activating mutants enabled us to perform a new set of epistasis tests that showed that Rim8, Rim9, and Rim21 function upstream of both Rim20 and Rim13 in the pathway. This conclusion is consistent with the report that Rim20 directly interacts with Rim101 (79) and also with a long-standing conjecture that calpain-like Rim13 is the protease directly catalyzing Rim101 processing. The three components placed upstream of Rim13 and Rim20, namely, putative membrane proteins Rim9 and Rim21, as well as Rim8, may constitute the pH-sensing machinery of the pathway (see below).

In contrast to the two pathway-activating mutants, *did4* and *vps24*, most other mutants defective in ESCRT components, i.e., *stp22*, *vps28*, *snf8*, *vps25*, *vps36*, *snf7*, and *vps20*, show impaired Rim101 processing, as well as LiCl sensitivity, with the only exception being *srn2* (see below). In this respect, these mutants share the phenotypes with *rim8*, *rim9*, *rim20*, *rim21*, and *rim13* mutants. Therefore, epistasis tests similar to those conducted for the *rim* mutations were performed for these ESCRT mutations. Both defective Rim101 processing and LiCl sensitivity of *stp22* and *vps28* were suppressed by *vps24*, those of *snf8* were moderately suppressed, and those of *vps25*, *vps36*, *snf7*, and *vps20* were not suppressed at all by *vps24*. These observations suggest that components of ESCRT-II, especially Vps25 and Vps36, and components of ESCRT-III, Snf7 and Vps20, play more important roles than those of ESCRT-I with respect to Rim101 processing. This is in line with previous genetic evidence indicating that ESCRT-II acts downstream of, and plays a more fundamental role than, ESCRT-I in MVB sorting (6).

Xu et al. reported that Rim101 processing is also deficient in an *srn2*Δ mutant (80). In contrast, an *srn2*Δ mutant was capable of Rim101 processing and tolerant of LiCl in our analysis, which was the only exception among mutants defective in ESCRT components (data not shown). Bowers et al. also reported that *srn2* mutants are tolerant of LiCl (13), but Eguez et al. reported that these mutants were sensitive (22). The reason for the discrepancy is currently unclear but may reflect somewhat milder phenotypes of *srn2* mutants relative to other mutants in ESCRT components, as observed in a higher restrictive temperature for growth, for example (data not shown).

Possible explanation for previously reported phenotypic differences among mutants defective in different ESCRT components. The disparity in Rim101 processing explains the difference in LiCl sensitivity among mutants defective in different ESCRT components. Full expression of *ENA1*, whose product is responsible for Li^+ efflux, requires processing of Rim101, and the fact hence is consistent with the observation that *did4* and *vps24* mutants are tolerant of LiCl and mutants defective in other ESCRT components sensitive (28, 40, 41). The disparity in Rim101 processing may also explain several previously unaddressed qualitative phenotypic differences among different ESCRT mutants. CPS, a selective cargo of MVB sorting, is reported to display different processing patterns in different ESCRT mutants (5). In *snf7*Δ and *vps20*Δ mutants, CPS was processed by the hydrolytic enzymes accumulated in the "class E" compartment, although in a slightly different pattern than occurs in wild-type cells. In contrast, CPS processing was impeded in *did4*Δ, *vps24*Δ, and *vps4*Δ mutants. The deficiency in CPS processing in *did4*Δ, *vps24*Δ, and *vps4*Δ mutants has been interpreted as a result of CPS being protected from proteolysis by sequestration or concentration in a compartment with a specific role for the Snf7-Vps20 subcomplex (5). Here we propose a different explanation. Lamb and Mitchell identified *PRB1*, which encodes a major vacuolar protease that catalyzes CPS processing, as a target gene for repression by Rim101 (40). Therefore, in *did4*Δ, *vps24*Δ, and *vps4*Δ mutants, proteolytic activity of Prb1p is likely low due to transcriptional repression by Rim101, and thus the low Prb1 activity will in turn result in deficient CPS processing. The previously reported differences in the sensitivity to Ca^{2+}, Mn^{2+}, and calcofluor white among mutants in different ESCRT components may also be attributed to the disparity in Rim101 processing (22, 66).

Mechanism for constitutive proteolytic processing of Rim101 in *did4*, *vps24*, and *vps4* mutants. Although all of the "class E" *vps* mutants share the same defective MVB sorting phenotype, only *did4*, *vps24*, and *vps4* mutants exhibit the constitutive proteolytic processing of Rim101. In contrast, the other mutants in ESCRT components, except for *srn2*, exhibit defective Rim101 processing. Furthermore, all non-ESCRT "class E" *vps* mutants except for *vps4* are normal in Rim101 processing. This difference in Rim101 processing among the "class E" *vps* mutants indicates that defective MVB sorting itself does not

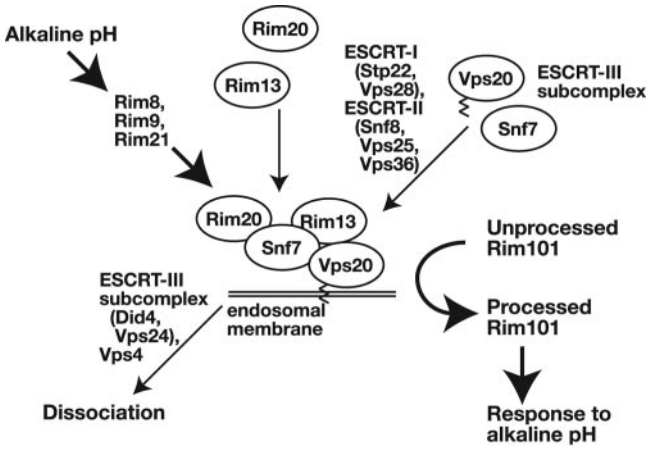

FIG. 5. Model for activation of Rim101 proteolytic processing by components of the Rim101 pathway; ESCRT-I, -II, and -III components; and Vps4 upon exposure to alkaline pH. See Discussion for a detailed explanation of this model.

cause constitutive Rim101 processing. Then, what is the mechanism that underlies constitutive Rim101 processing?

According to the seminal studies on the ESCRT complexes by Emr and coworkers, *did4*, *vps24*, and *vps4* mutants commonly accumulate the Vps20-Snf7 subcomplex of ESCRT-III on the endosomal membrane (5, 8, 9). This accumulation is not observed in other mutants in ESCRT components (5). In contrast, Emr and coworkers have shown that many other mutants in ESCRT components are defective in formation and endosomal membrane loading of ESCRT-III. Our results reveal a consistent correlation between the reported membrane loading of Vps20-Snf7 and Rim101 processing. First, not only defects in Vps20 or Snf7 itself but also defects in ESCRT-I or ESCRT-II have been shown to prevent loading of Vps20-Snf7 onto the endosomal membrane (6). Concomitantly, mutants in ESCRT-I or ESCRT-II components are defective in Rim101 processing, with the sole exception of *srn2* (see above). Second, in a *vps4* background, ESCRT-II is required but ESCRT-I is not required for loading of Vps20-Snf7 on the endosomal membrane (6). This again is in good agreement with the results of our epistasis tests that show that defective Rim101 processing of the ESCRT-I mutants *stp22* and *vps28* is suppressed by *vps24* but that of ESCRT-II mutants *vps25* and *vps36* is not. An exceptional component of ESCRT-II in this respect is Snf8, in that defective Rim101 processing in a *snf8* mutant is partially suppressed by *vps24*. Because possible accumulation of Vps20-Snf7 on the endosomal membrane in *snf8 did4*, *snf8 vps24*, or *snf8 vps4* double mutants has not been examined, this point requires further study.

In light of these observations, we propose that either formation or the endosomal membrane loading of the Vps20-Snf7 subcomplex activates proteolytic processing of Rim101. On the other hand, it has already been suggested that a complex of Rim20-Snf7-Rim13 is responsible for catalyzing proteolytic processing of Rim101 (79). Extending this model, we then propose the following mechanism for constitutive proteolytic processing of Rim101 in *did4*, *vps24*, and *vps4* mutants (Fig. 5). In these mutants, the Vps20-Snf7 subcomplex of ESCRT-III accumulates on the endosomal membrane. To this subcomplex, Rim20 and Rim13 are recruited to form a higher-order complex consisting of Rim20-(Vps20-Snf7)-Rim13 through an interaction between Rim20 and Snf7 and between Snf7 and Rim13. The formation of this complex, we propose, promotes proteolytic processing of Rim101 by recruiting Rim101 through interaction with Rim20 and thereby presenting it to activated Rim13. To test this model, localization of components of the Rim101 pathway and the ESCRT complexes need to be determined at different pH values or in various mutants of ESCRT components.

vps4 mutants exhibit constitutive processing of Rim101, although the extent of processing seems moderate relative to what was observed in *did4* and *vps24* mutants. This may be explained as follows. In *vps4* mutants, the Did4-Vps24 subcomplex is loaded onto the Vps20-Snf7 subcomplex on the endosomal membrane (5, 9) and potentially competes with Rim20 and/or Rim13 for binding to Vps20-Snf7. In contrast, in *did4* and *vps24* mutants Did4-Vps24 does not exist, and thus Vps20-Snf7 is fully available for binding to Rim20 and/or Rim13.

Mechanism for alkaline-responsive proteolytic processing of Rim101. By extending the above discussion on constitutive processing of Rim101 in *did4*Δ, *vps24*Δ, and *vps4*Δ mutants to the alkaline pH-responsive processing of Rim101 in wild-type cells, we propose that a similar mechanism operates in both processes. In this model, a complex of Rim20-(Vps20-Snf7)-Rim13 forms under conditions of alkaline pH in a Rim8-, Rim9-, and Rim21-dependent manner (Fig. 5). The concrete mechanism by which Rim8, Rim9, and Rim21 promote formation of the Rim20-(Vps20-Snf7)-Rim13 complex remains to be determined, although it is clear that formation of the complex also requires both ESCRT-I and ESCRT-II. Even in *did4* or *vps24* mutants, Rim8, Rim9, and Rim21 still play some role in facilitating Rim101 processing, because defective Rim101 processing in *rim8*, *rim9*, and *rim21* mutants is not fully restored, even when suppressed by *did4* or *vps24*: in *did4* cells for example, the extent of Rim101 processing is more pronounced than in *rim8 did4* cells. One speculative possibility is that, by mimicking cargo proteins for MVB sorting, either Rim9 or Rim21 recruits ESCRT-I onto the endosomal membrane, thereby promoting formation of the Rim20-(Vps20-Snf7)-Rim13 complex under alkaline conditions. If the recruitment of ESCRT-I depends on ubiquitination of Rim9 or Rim21, as is the case for known cargo proteins, the ubiquitination should occur in an alkaline pH-dependent manner. This point remains to be determined. Stimulation-dependent ubiquitination and endosomal sorting are common modes of desensitization of membrane receptors/sensors (34), and this model proposes a variant of this common mechanism that makes use of recruitment of ESCRT complexes not for downregulation, but for signaling itself.

Physiological significance of the link between the Rim101 pathway and MVB sorting. We have shown a close relationship between the Rim101 pathway and MVB sorting. What is the physiological significance of this link? MVB sorting requires a pH gradient across the endosomal membrane. In fact, efficient sorting of vacuolar proteins is impaired under alkaline conditions (36). In addition, mutational or pharmacological inactivation of the vacuolar H^+-ATPase, which disrupt acidification of the vacuolar, and perhaps the endosomal, compartment also causes defective vacuolar protein sorting (10, 36, 52, 64, 75, 81).

The defects in MVB sorting under these conditions may arise from impaired formation of MVB. Consistent with this, Matsuo et al. reported that formation of MVB-like liposomes in an in vitro system required a pH gradient across the liposome membrane that reproduced the in vivo lumenal acidic pH of the endosome (49). If impairment in MVB formation under alkaline conditions blocks the process of MVB sorting after the step of ESCRT-III loading, as in *did4*, *vps24*, or *vps4* mutants, formation of the active Rim20-(Vps20-Snf7)-Rim13 complex would be promoted under these conditions. This implies that failure to maintain a pH gradient across the endosomal membrane under alkaline conditions can be coupled with activation of the Rim101 pathway. This will ensure, in theory at least, the appropriate response of the Rim101 pathway to raises in environmental pH.

Finally, it should be noted that all of the components of the aforementioned protease complex have one or more mammalian homologs. Rim13 is the only calpain homolog in yeast, whereas humans have 14 genes for calpains, including PalBH/calpain 7, which is most similar to Rim13 (23, 24, 26, 70). The human homologs of Rim20, Snf7, and Vps20 are Alix/AIP1, CHMP4/hSnf7, and hVps20, respectively (32, 51, 58, 76). The existence of these homologs suggests that a similar mechanism might operate in mammalian cells. The possibility of calpain functioning at the membranes is also implied by the present study. Indeed, recent studies have shown that conventional calpains localize and function at the endoplasmic reticulum and the lysosome (11, 57, 71). Elucidation of the mechanism that regulates activation of the Rim101 pathway should shed further light on the biology of calpains in general.

ACKNOWLEDGMENTS

We thank Fred Winston, Janice Kranz, Konnie Holm, Mark Longtine, Yoichi Noda, and Koji Yoda for yeast strains and plasmids. We also thank Eugene Futai, Koichi Suzuki, and all of the members of the Maeda laboratory for help, advice, and discussion.

This study was supported in part by a Grant-in-Aid for Scientific Research on Priority Areas (KAKENHI 14086203) from the Ministry of Education, Culture, Sports, Science, and Technology (MEXT) and a grant (no. 0349) from the Salt Science Research Foundation (both to T.M.).

REFERENCES

1. **Amerik, A. Y., J. Nowak, S. Swaminathan, and M. Hochstrasser.** 2000. The Doa4 deubiquitinating enzyme is functionally linked to the vacuolar protein-sorting and endocytic pathways. Mol. Biol. Cell **11:**3365–3380.
2. **Arst, H. N., E. Bignell, and J. Tilburn.** 1994. Two new genes involved in signalling ambient pH in *Aspergillus nidulans*. Mol. Gen. Genet. **245:**787–790.
3. **Arst, H. N., and M. A. Peñalva.** 2003. pH regulation in *Aspergillus* and parallels with higher eukaryotic regulatory systems. Trends Genet. **19:** 224–231.
4. **Ausubel, F. M., R. Brent, R. E. Kingston, D. D. Moore, J. G. Seidman, J. A. Smith, and K. Struhl.** 1988. Current protocols in molecular biology. John Wiley & Sons, Inc., New York, N.Y.
5. **Babst, M., D. J. Katzmann, E. J. Estepa-Sabal, T. Meerloo, and S. D. Emr.** 2002. ESCRT-III: an endosome-associated heterooligomeric protein complex required for MVB sorting. Dev. Cell **3:**271–282.
6. **Babst, M., D. J. Katzmann, W. B. Snyder, B. Wendland, and S. D. Emr.** 2002. Endosome-associated complex, ESCRT-II, recruits transport machinery for protein sorting at the multivesicular body. Dev. Cell **3:**283–289.
7. **Babst, M., G. Odorizzi, E. J. Estepa, and S. D. Emr.** 2000. Mammalian tumor susceptibility gene 101 (TSG101) and the yeast homologue, Vps23p, both function in late endosomal trafficking. Traffic **1:**248–258.
8. **Babst, M., T. K. Sato, L. M. Banta, and S. D. Emr.** 1997. Endosomal transport function in yeast requires a novel AAA-type ATPase, Vps4p. EMBO J. **16:**1820–1831.
9. **Babst, M., B. Wendland, E. J. Estepa, and S. D. Emr.** 1998. The Vps4p AAA ATPase regulates membrane association of a Vps protein complex required for normal endosome function. EMBO J. **17:**2982–2993.
10. **Banta, L. M., J. S. Robinson, D. J. Klionsky, and S. D. Emr.** 1988. Organelle assembly in yeast: characterization of yeast mutants defective in vacuolar biogenesis and protein sorting. J. Cell Biol. **107:**1369–1383.
11. **Bianchi, L., B. Gerstbrein, C. Frøkj(ligae)r-Jensen, D. C. Royal, G. Mukherjee, M. A. Royal, J. Xue, W. R. Schafer, and M. Driscoll.** 2004. The neurotoxic MEC-4(d) DEG/ENaC sodium channel conducts calcium: implications for necrosis initiation. Nat. Neurosci. **7:**1337–1344.
12. **Bonneu, M., M. Crouzet, M. Urdaci, and M. Aigle.** 1991. Direct detection of yeast mutants with reduced viability on plates by erythrosine B staining. Anal. Biochem. **193:**225–230.
13. **Bowers, K., J. Lottridge, S. B. Helliwell, L. M. Goldthwaite, J. P. Luzio, and T. H. Stevens.** 2004. Protein-protein interactions of ESCRT complexes in the yeast *Saccharomyces cerevisiae*. Traffic **5:**194–210.
14. **Brachmann, C. B., A. Davies, G. J. Cost, E. Caputo, J. Li, P. Hieter, and J. D. Boeke.** 1998. Designer deletion strains derived from *Saccharomyces cerevisiae* S288C: a useful set of strains and plasmids for PCR-mediated gene disruption and other applications. Yeast **14:**115–132.
15. **Burd, C. G., and S. D. Emr.** 1998. Phosphatidylinositol(3)-phosphate signaling mediated by specific binding to RING FYVE domains. Mol. Cell **2:** 157–162.
16. **Burke, D., D. Dawson, and T. Stearns.** 2000. Methods in yeast genetics: a Cold Spring Harbor Laboratory course manual. Cold Spring Harbor Laboratory Press, Cold Spring Harbor, N.Y.
17. **Caddick, M. X., A. G. Brownlee, and H. N. Arst.** 1986. Regulation of gene expression by pH of the growth medium in *Aspergillus nidulans*. Mol. Gen. Genet. **203:**346–353.
18. **Davis, D., R. B. Wilson, and A. P. Mitchell.** 2000. *RIM101*-dependent and-independent pathways govern pH responses in *Candida albicans*. Mol. Cell. Biol. **20:**971–978.
19. **Denison, S. H., S. Negrete-Urtasun, J. M. Mingot, J. Tilburn, W. A. Mayer, A. Goel, E. A. Espeso, M. A. Peñalva, and H. N. Arst.** 1998. Putative membrane components of signal transduction pathways for ambient pH regulation in *Aspergillus* and meiosis in *Saccharomyces* are homologous. Mol. Microbiol. **30:**259–264.
20. **Denison, S. H., M. Orejas, and H. N. Arst.** 1995. Signaling of ambient pH in *Aspergillus* involves a cysteine protease. J. Biol. Chem. **270:**28519–28522.
21. **Díez, E., J. Alvaro, E. A. Espeso, L. Rainbow, T. Suárez, J. Tilburn, H. N. Arst, and M. A. Peñalva.** 2002. Activation of the *Aspergillus* PacC zinc finger transcription factor requires two proteolytic steps. EMBO J. **21:**1350–1359.
22. **Eguez, L., Y. S. Chung, A. Kuchibhatla, M. Paidhungat, and S. Garrett.** 2004. Yeast Mn^{2+} transporter, Smf1p, is regulated by ubiquitin-dependent vacuolar protein sorting. Genetics **167:**107–117.
23. **Franz, T., M. Vingron, T. Boehm, and T. N. Dear.** 1999. Capn7: a highly divergent vertebrate calpain with a novel C-terminal domain. Mamm. Genome **10:**318–321.
24. **Futai, E., T. Kubo, H. Sorimachi, K. Suzuki, and T. Maeda.** 2001. Molecular cloning of PalBH, a mammalian homologue of the *Aspergillus* atypical calpain PalB. Biochim. Biophys. Acta **1517:**316–319.
25. **Futai, E., T. Maeda, H. Sorimachi, K. Kitamoto, S. Ishiura, and K. Suzuki.** 1999. The protease activity of a calpain-like cysteine protease in *Saccharomyces cerevisiae* is required for alkaline adaptation and sporulation. Mol. Gen. Genet. **260:**559–568.
26. **Goll, D. E., V. F. Thompson, H. Li, W. Wei, and J. Cong.** 2003. The calpain system. Physiol. Rev. **83:**731–801.
27. **Gonzalez-Lopez, C. I., R. Szabo, S. Blanchin-Roland, and C. Gaillardin.** 2002. Genetic control of extracellular protease synthesis in the yeast *Yarrowia lipolytica*. Genetics **160:**417–427.
28. **Haro, R., B. Garciadeblas, and A. Rodríguez-Navarro.** 1991. A novel P-type ATPase from yeast involved in sodium transport. FEBS Lett. **291:**189–191.
29. **Hong, S. J., Y. S. Yi, S. S. Koh, O. K. Park, and H. S. Kang.** 1998. Isolation of an extragenic suppressor of the *rna1-1* mutation in *Saccharomyces cerevisiae*. Mol. Gen. Genet. **259:**404–413.
30. **Ito, T., T. Chiba, R. Ozawa, M. Yoshida, M. Hattori, and Y. Sakaki.** 2001. A comprehensive two-hybrid analysis to explore the yeast protein interactome. Proc. Natl. Acad. Sci. USA **98:**4569–4574.
31. **Jones, E. W., G. C. Webb, and M. A. Hiller.** 1997. Biogenesis and function of the yeast vacuole, p. 363–470. *In* J. R. Pringle, J. R. Broach, and E. W. Jones (ed.), The molecular and cellular biology of the yeast *Saccharomyces*, volume 3: cell cycle and cell biology. Cold Spring Harbor Laboratory Press, Cold Spring Harbor, N.Y.
32. **Katoh, K., H. Shibata, H. Suzuki, A. Nara, K. Ishidoh, E. Kominami, T. Yoshimori, and M. Maki.** 2003. The ALG-2-interacting protein Alix associates with CHMP4b, a human homologue of yeast Snf7 that is involved in multivesicular body sorting. J. Biol. Chem. **278:**39104–39113.
33. **Katzmann, D. J., M. Babst, and S. D. Emr.** 2001. Ubiquitin-dependent sorting into the multivesicular body pathway requires the function of a conserved endosomal protein sorting complex, ESCRT-I. Cell **106:**145–155.
34. **Katzmann, D. J., G. Odorizzi, and S. D. Emr.** 2002. Receptor downregulation and multivesicular-body sorting. Nat. Rev. Mol. Cell Biol. **3:**893–905.
35. **Katzmann, D. J., C. J. Stefan, M. Babst, and S. D. Emr.** 2003. Vps27 recruits ESCRT machinery to endosomes during MVB sorting. J. Cell Biol. **162:** 413–423.

36. **Klionsky, D. J., H. Nelson, and N. Nelson.** 1992. Compartment acidification is required for efficient sorting of proteins to the vacuole in *Saccharomyces cerevisiae*. J. Biol. Chem. **267:**3416–3422.
37. **Kranz, A., A. Kinner, and R. Kölling.** 2001. A family of small coiled-coil-forming proteins functioning at the late endosome in yeast. Mol. Biol. Cell **12:**711–723.
38. **Kranz, J. E., and C. Holm.** 1990. Cloning by function: an alternative approach for identifying yeast homologs of genes from other organisms. Proc. Natl. Acad. Sci. USA **87:**6629–6633.
39. **Kullas, A. L., M. Li, and D. A. Davis.** 2004. Snf7p, a component of the ESCRT-III protein complex, is an upstream member of the *RIM101* pathway in *Candida albicans*. Eukaryot. Cell **3:**1609–1618.
40. **Lamb, T. M., and A. P. Mitchell.** 2003. The transcription factor Rim101p governs ion tolerance and cell differentiation by direct repression of the regulatory genes *NRG1* and *SMP1* in *Saccharomyces cerevisiae*. Mol. Cell. Biol. **23:**677–686.
41. **Lamb, T. M., W. Xu, A. Diamond, and A. P. Mitchell.** 2001. Alkaline response genes of *Saccharomyces cerevisiae* and their relationship to the *RIM101* pathway. J. Biol. Chem. **276:**1850–1856.
42. **Lambert, M., S. Blanchin-Roland, F. Le Louedec, A. Lepingle, and C. Gaillardin.** 1997. Genetic analysis of regulatory mutants affecting synthesis of extracellular proteinases in the yeast *Yarrowia lipolytica*: identification of a *RIM101/pacC* homolog. Mol. Cell. Biol. **17:**3966–3976.
43. **Li, M., S. J. Martin, V. M. Bruno, A. P. Mitchell, and D. A. Davis.** 2004. *Candida albicans* Rim13p, a protease required for Rim101p processing at acidic and alkaline pHs. Eukaryot. Cell **3:**741–751.
44. **Li, W., and A. P. Mitchell.** 1997. Proteolytic activation of Rim1p, a positive regulator of yeast sporulation and invasive growth. Genetics **145:**63–73.
45. **Li, Y., T. Kane, C. Tipper, P. Spatrick, and D. D. Jenness.** 1999. Yeast mutants affecting possible quality control of plasma membrane proteins. Mol. Cell. Biol. **19:**3588–3599.
46. **Longtine, M. S., A. McKenzie, D. J. Demarini, N. G. Shah, A. Wach, A. Brachat, P. Philippsen, and J. R. Pringle.** 1998. Additional modules for versatile and economical PCR-based gene deletion and modification in *Saccharomyces cerevisiae*. Yeast **14:**953–961.
47. **Luo, W., and A. Chang.** 2000. An endosome-to-plasma membrane pathway involved in trafficking of a mutant plasma membrane ATPase in yeast. Mol. Biol. Cell **11:**579–592.
48. **Maccheroni, W., G. S. May, N. M. Martinez-Rossi, and A. Rossi.** 1997. The sequence of *palF*, an environmental pH response gene in *Aspergillus nidulans*. Gene **194:**163–167.
49. **Matsuo, H., J. Chevallier, N. Mayran, I. Le Blanc, C. Ferguson, J. Fauré, N. S. Blanc, S. Matile, J. Dubochet, R. Sadoul, R. G. Parton, F. Vilbois, and J. Gruenberg.** 2004. Role of LBPA and Alix in multivesicular liposome formation and endosome organization. Science **303:**531–534.
50. **Mingot, J. M., J. Tilburn, E. Diez, E. Bignell, M. Orejas, D. A. Widdick, S. Sarkar, C. V. Brown, M. X. Caddick, E. A. Espeso, H. N. Arst, and M. A. Peñalva.** 1999. Specificity determinants of proteolytic processing of *Aspergillus* PacC transcription factor are remote from the processing site, and processing occurs in yeast if pH signaling is bypassed. Mol. Cell. Biol. **19:**1390–1400.
51. **Missotten, M., A. Nichols, K. Rieger, and R. Sadoul.** 1999. Alix, a novel mouse protein undergoing calcium-dependent interaction with the apoptosis-linked-gene 2 (ALG-2) protein. Cell Death Differ. **6:**124–129.
52. **Morano, K. A., and D. J. Klionsky.** 1994. Differential effects of compartment deacidification on the targeting of membrane and soluble proteins to the vacuole in yeast. J. Cell Sci. **107:**2813–2824.
53. **Negrete-Urtasun, S., S. H. Denison, and H. N. Arst.** 1997. Characterization of the pH signal transduction pathway gene *palA* of *Aspergillus nidulans* and identification of possible homologs. J. Bacteriol. **179:**1832–1835.
54. **Negrete-Urtasun, S., W. Reiter, E. Diez, S. H. Denison, J. Tilburn, E. A. Espeso, M. A. Peñalva, and H. N. Arst.** 1999. Ambient pH signal transduction in *Aspergillus*: completion of gene characterization. Mol. Microbiol. **33:**994–1003.
55. **Orejas, M., E. A. Espeso, J. Tilburn, S. Sarkar, H. N. Arst, and M. A. Peñalva.** 1995. Activation of the *Aspergillus* PacC transcription factor in response to alkaline ambient pH requires proteolysis of the carboxy-terminal moiety. Genes Dev. **9:**1622–1632.
56. **Papa, F. R., and M. Hochstrasser.** 1993. The yeast *DOA4* gene encodes a deubiquitinating enzyme related to a product of the human *tre-2* oncogene. Nature **366:**313–319.
57. **Pattni, K., T. H. Millard, and G. Banting.** 2003. Calpain cleavage of the B isoform of Ins(1,4,5)P_3 3-kinase separates the catalytic domain from the membrane anchoring domain. Biochem. J. **375:**643–651.
58. **Peck, J. W., E. T. Bowden, and P. D. Burbelo.** 2004. Structure and function of human Vps20 and Snf7 proteins. Biochem. J. **377:**693–700.
59. **Peñalva, M. A., and H. N. Arst.** 2002. Regulation of gene expression by ambient pH in filamentous fungi and yeasts. Microbiol. Mol. Biol. Rev. **66:**426–446.
60. **Piper, R. C., A. A. Cooper, H. Yang, and T. H. Stevens.** 1995. *VPS27* controls vacuolar and endocytic traffic through a prevacuolar compartment in *Saccharomyces cerevisiae*. J. Cell Biol. **131:**603–617.
61. **Porta, A., A. M. Ramon, and W. A. Fonzi.** 1999. *PRR1*, a homolog of *Aspergillus nidulans palF*, controls pH-dependent gene expression and filamentation in *Candida albicans*. J. Bacteriol. **181:**7516–7523.
62. **Ramon, A. M., A. Porta, and W. A. Fonzi.** 1999. Effect of environmental pH on morphological development of *Candida albicans* is mediated via the PacC-related transcription factor encoded by *PRR2*. J. Bacteriol. **181:**7524–7530.
63. **Rieder, S. E., L. M. Banta, K. Köhrer, J. M. McCaffery, and S. D. Emr.** 1996. Multilamellar endosome-like compartment accumulates in the yeast *vps28* vacuolar protein sorting mutant. Mol. Biol. Cell **7:**985–999.
64. **Rothman, J. H., C. T. Yamashiro, C. K. Raymond, P. M. Kane, and T. H. Stevens.** 1989. Acidification of the lysosome-like vacuole and the vacuolar H^+-ATPase are deficient in two yeast mutants that fail to sort vacuolar proteins. J. Cell Biol. **109:**93–100.
65. **Serrano, R., A. Ruiz, D. Bernal, J. R. Chambers, and J. Ariño.** 2002. The transcriptional response to alkaline pH in *Saccharomyces cerevisiae*: evidence for calcium-mediated signalling. Mol. Microbiol. **46:**1319–1333.
66. **Shiflett, S. L., D. M. Ward, D. Huynh, M. B. Vaughn, J. C. Simmons, and J. Kaplan.** 2004. Characterization of Vta1p, a class E Vps protein in *Saccharomyces cerevisiae*. J. Biol. Chem. **279:**10982–10990.
67. **Shih, S. C., D. J. Katzmann, J. D. Schnell, M. Sutanto, S. D. Emr, and L. Hicke.** 2002. Epsins and Vps27p/Hrs contain ubiquitin-binding domains that function in receptor endocytosis. Nat. Cell Biol. **4:**389–393.
68. **Su, S. S., and A. P. Mitchell.** 1993. Identification of functionally related genes that stimulate early meiotic gene expression in yeast. Genetics **133:**67–77.
69. **Su, S. S., and A. P. Mitchell.** 1993. Molecular characterization of the yeast meiotic regulatory gene, *RIM1*. Nucleic Acids Res. **21:**3789–3797.
70. **Suzuki, K., S. Hata, Y. Kawabata, and H. Sorimachi.** 2004. Structure, activation, and biology of calpain. Diabetes **53**(Suppl. 1)**:**S12–S18.
71. **Syntichaki, P., K. Xu, M. Driscoll, and N. Tavernarakis.** 2002. Specific aspartyl and calpain proteases are required for neurodegeneration in *Caenorhabditis elegans*. Nature **419:**939–944.
72. **Tilburn, J., S. Sarkar, D. A. Widdick, E. A. Espeso, M. Orejas, J. Mungroo, M. A. Peñalva, and H. N. Arst.** 1995. The *Aspergillus* PacC zinc finger transcription factor mediates regulation of both acid- and alkaline-expressed genes by ambient pH. EMBO J. **14:**779–790.
73. **Tréton, B., S. Blanchin-Roland, M. Lambert, A. Lépingle, and C. Gaillardin.** 2000. Ambient pH signalling in ascomycetous yeasts involves homologues of the *Aspergillus nidulans* genes *palF* and *paIH*. Mol. Gen. Genet. **263:**505–513.
74. **Tu, J., L. G. Vallier, and M. Carlson.** 1993. Molecular and genetic analysis of the *SNF7* gene in *Saccharomyces cerevisiae*. Genetics **135:**17–23.
75. **Umemoto, N., T. Yoshihisa, R. Hirata, and Y. Anraku.** 1990. Roles of the *VMA3* gene product, subunit c of the vacuolar membrane H^+-ATPase on vacuolar acidification and protein transport. A study with *VMA3*-disrupted mutants of *Saccharomyces cerevisiae*. J. Biol. Chem. **265:**18447–18453.
76. **Vito, P., L. Pellegrini, C. Guiet, and L. D'Adamio.** 1999. Cloning of AIP1, a novel protein that associates with the apoptosis-linked gene ALG-2 in a Ca^{2+}-dependent reaction. J. Biol. Chem. **274:**1533–1540.
77. **Winston, F., C. Dollard, and S. L. Ricupero-Hovasse.** 1995. Construction of a set of convenient *Saccharomyces cerevisiae* strains that are isogenic to S288C. Yeast **11:**53–55.
78. **Winzeler, E. A., D. D. Shoemaker, A. Astromoff, H. Liang, K. Anderson, B. Andre, R. Bangham, R. Benito, J. D. Boeke, H. Bussey, A. M. Chu, C. Connelly, K. Davis, F. Dietrich, S. W. Dow, M. El Bakkoury, F. Foury, S. H. Friend, E. Gentalen, G. Giaever, J. H. Hegemann, T. Jones, M. Laub, H. Liao, and R. W. Davis.** 1999. Functional characterization of the *Saccharomyces cerevisiae* genome by gene deletion and parallel analysis. Science **285:**901–906.
79. **Xu, W., and A. P. Mitchell.** 2001. Yeast PalA/AIP1/Alix homolog Rim20p associates with a PEST-like region and is required for its proteolytic cleavage. J. Bacteriol. **183:**6917–6923.
80. **Xu, W., F. J. Smith, R. Subaran, and A. P. Mitchell.** 2004. Multivesicular body-ESCRT components function in pH response regulation in *Saccharomyces cerevisiae* and *Candida albicans*. Mol. Biol. Cell **15:**5528–5537.
81. **Yamashiro, C. T., P. M. Kane, D. F. Wolczyk, R. A. Preston, and T. H. Stevens.** 1990. Role of vacuolar acidification in protein sorting and zymogen activation: a genetic analysis of the yeast vacuolar proton-translocating ATPase. Mol. Cell. Biol. **10:**3737–3749.
82. **Yeghiayan, P., J. Tu, L. G. Vallier, and M. Carlson.** 1995. Molecular analysis of the *SNF8* gene of *Saccharomyces cerevisiae*. Yeast **11:**219–224.